Performance of Generalized Multicarrier DS-CDMA Over Nakagami-m Fading Channels

Lie-Liang Yang, *Member, IEEE,* and Lajos Hanzo, *Senior Member, IEEE*

***Abstract*—A class of generalized multicarrier direct sequence code-division multiple-access (MC DS-CDMA) schemes is defined and its performance is considered over multipath Nakagami-m fading channels. The spacing between two adjacent subcarriers of the generalized MC DS-CDMA is a variable, allowing us to gain insight into the effects of the spacing on the bit error rate (BER) performance of MC DS-CDMA systems. This generalized MC DS-CDMA scheme includes the subclasses of multitone DS-CDMA and orthogonal MC DS-CDMA as special cases. We present a unified analytical framework for determining the exact average BER of the generalized MC DS-CDMA system over generalized multipath Nakagami-m fading channels. The optimum spacing of the MC DS-CDMA system required for achieving the minimum BER is investigated and the BER performance of the system having optimum spacing is evaluated. The resultant BER is compared with that of both multitone DS-CDMA and orthogonal MC DS-CDMA.**

I. Introduction

RECENTLY, a novel class of code-division multiple-access (CDMA) systems based on the combination of CDMA schemes and orthogonal frequency division multiplexing (OFDM)—which is referred to as multicarrier CDMA (MC-CDMA)—has drawn a lot of attention [1]–[14]. MC-CDMA is capable of supporting high data rate services over hostile radio channels. The modulated signal can be generated with the aid of the fast Fourier transform (FFT) at the cost of low receiver complexity.

In these MC-CDMA schemes, the transmitter of both multitone based direct-sequence CDMA [3] (multitone DS-CDMA) and that of orthogonal multicarrier DS-CDMA (MC DS-CDMA) [2], [5] spreads the serial-to-parallel converted data streams using a given spreading code in the time domain. In a multitone DS-CDMA system the subcarrier frequencies are chosen to be orthogonal harmonics of each other with minimum frequency separation among them before DS spreading [3], which is expressed as

$$\int_0^{T_s} \cos(2\pi f_i t+\phi_i)\cdot\cos(2\pi f_j t+\phi_j)\,dt = 0, \quad \text{for } i \neq j \quad (1)$$

where T_s represents the symbol duration of the multitone DS-CDMA signal, while $\{f_i\}$ and $\{\phi_i\}$ are the subcarrier frequencies and initial phases, respectively. Therefore, in multitone DS-CDMA systems, the spacing Δ between two adjacent subcarrier frequencies is $\Delta = 1/T_s$. The subcarrier frequencies hence take the form of $f_0 + i/T_s$ for $i = 0, 1, \ldots, U-1$, where U is the number of subcarriers and f_0 is the fundamental frequency. By contrast, in an orthogonal MC DS-CDMA system, the subcarrier frequencies are chosen to satisfy the orthogonality condition with the minimum possible frequency separation after DS spreading [1], [2], [5], which can be expressed as

$$\int_0^{T_c} \cos(2\pi f_i t+\phi_i)\cdot\cos(2\pi f_j t+\phi_j)\,dt = 0, \quad \text{for } i \neq j \quad (2)$$

which implies that the spacing Δ between two adjacent subcarrier frequencies is $\Delta = 1/T_c$, where T_c is the chip duration of the DS spreading codes and the subcarrier frequencies take the form of $f_0 + i/T_c$ for $i = 0, 1, \ldots, U-1$.

Let $N_e = T_s/T_c$ be the spreading gain of the DS-spread subcarrier signals. Furthermore, we assume that each subcarrier's modulated signal has the same "null-to-null" bandwidth of $2/T_c$. Then, it can be readily shown that the condition of (1) actually includes the orthogonality condition of both the multitone and the orthogonal MC DS-CDMA schemes. This observation can be readily justified by letting the subcarrier frequencies $f_i = f_0 + iN_e/T_s = f_0 + i/T_c$ for $i = 0, 1, \ldots, U-1$ in (1). Furthermore, it can be readily shown that the orthogonality condition of (1) is obeyed, whenever the spacing Δ takes the form of $\Delta = \lambda/T_s$, $\lambda = 1, 2, \ldots$, where λ is referred to as the normalized spacing between two adjacent subcarriers. The MC DS-CDMA scheme belongs to the family of multitone DS-CDMA arrangements, if $\lambda = 1$, while to the class of orthogonal MC DS-CDMA systems, if $\lambda = N_e$. Furthermore, there exists no overlap between the main lobes of the modulated subcarrier signals after DS spreading, when $\lambda = 2N_e$, which is the bandwidth requirement of the MC DS-CDMA system proposed in [4].

Based on the above observations, both the multitone DS-CDMA system and the orthogonal MC DS-CDMA system can be viewed as a member of the class of generalized multicarrier DS-CDMA systems having arbitrary subcarrier spacing of $\lambda \in \{1, 2, \ldots, \}$. Hence, the above generalized MC DS-CDMA system model includes a number of specific MC DS-CDMA schemes. Furthermore, based on the analysis of this general model, the results generated can be extended to different MC DS-CDMA systems by simply varying a single parameter, namely λ. Finally, the subcarrier spacing λ

Paper approved by Y. Li, the Editor for Wireless Communication Theory of the IEEE Communications Society. Manuscript received May 1, 2000; revised January 2, 2001, and October 31, 2001. This work was supported in the framework of the IST Project IST-1999-12070 TRUST, which is supported in part by the European Union. This paper was presented in part at Globecom 2001, San Antonio, TX, Nov. 25–29, 2001.

The authors are with the Department of Electronics and Computer Science, University of Southampton, SO17 1BJ, UK (e-mail: lly@ecs.soton.ac.uk; lh@ecs.soton.ac.uk).

Publisher Item Identifier S 0090-6778(02)05560-5.

can be optimized according to specific design requirements tailored to the communication environments encountered, in order to achieve the optimum performance in terms of λ. For example, for a given total system bandwidth, λ can be optimized, in order to minimize the multiuser interference, since it has an influence on both the overlap of the modulated subcarrier signals and on the processing gain. In this context a clear trade-off exists between the overlap and the processing gain. On the one hand, if λ is low—for example $\lambda = 1$—in the context of multitone DS-CDMA, then a subcarrier signal will overlap with a high number of subcarrier signals of both the same user and with those of the interfering users. On the other hand, given a total bandwidth and a low value of λ, a high spreading gain can be maintained, which leads to the reduction of the multiuser interference. By contrast, if λ is high—for example, $\lambda = 2N_e$—which means that there exists no spectral overlap between the main lobes of the subcarrier signals, then the modulated subcarrier signals benefit from a low interference inflicted by the other subcarrier signals of both the reference and the interfering users. However, in this case, the spreading gain of each subcarrier signal is low, which leads to an increased multiuser interference. The influence of the subcarrier spacing λ on both the spreading gain and on the spectral overlap of the subcarrier signals highlights that there exists an optimum spacing λ_{opt} which minimizes the multiuser interference inflicted upon each of the subcarrier signals. Another example in the context of optimizing λ is that the subcarrier spacing λ can be adjusted for matching the receiver's requirements. For example, assuming that the receiver employs a three-finger RAKE receiver, a specific spacing λ can be selected such that the number of resolvable paths becomes three in the propagation environment encountered. In this case, the highest possible diversity gain is achieved, since the receiver can combine all the energy scattered over the multipath components. The adjustment of the subcarrier-spacing parameter λ can be implemented as follows. If there exists a low-delay feedback channel between the receiver and the transmitter—which is the case in the existing wireless systems, such as in the 3G systems—the parameter λ as well as the corresponding chip-rate of the spreading sequences can be reconfigured according to the near-instantaneous channel quality. However, if the near-instantaneous channel quality cannot be readily estimated, the subcarrier-spacing parameter λ can be designed according to the typical channel characteristics encountered—such as indoor, outdoor, urban, rural, etc., environments.

In this paper, the performance of the above generalized MC DS-CDMA system is evaluated over the range of Nakagami-m multipath fading channels. This generic channel model is used, since the Nakagami-m distribution is a generalized distribution, which often gives the best fit to land-mobile and indoor-mobile multipath propagation environments, as well as to scintillating ionospheric radio links [15]. A good fit to these widely varying propagation scenarios is achieved by varying the single parameter of m in the Nakagami-m distribution [13]–[27]. Furthermore, the Nakagami-m distribution offers features of analytical convenience, as it has been shown in numerous treatises [13]–[27] and also in this contribution.

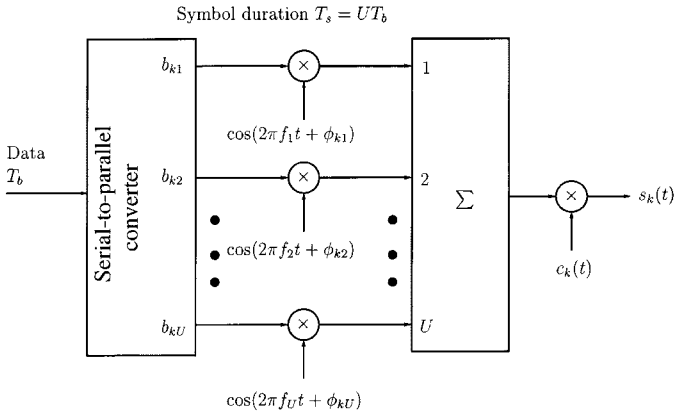

Fig. 1. The kth user's transmitter schematic for the generalized MC DS-CDMA system.

The remainder of this paper is organized as follows. In the next section, the above generalized MC DS-CDMA system as well as the Nakagami-m fading channel model are described in more detail. In Section III, we analyze the statistics of the decision variables. In Section IV the probability of error is derived for the generalized MC DS-CDMA system, and then this result is studied in specific scenarios. Our numerical results and comparisons are outlined in Section V, and finally, our conclusions are offered in Section VI.

II. Generalized Multicarrier DS-CDMA Systems

A. Transmitted Signal

The transmitter schematic of the kth user is shown in Fig. 1 for the generalized MC DS-CDMA system, which is similar to that of a multitone DS-CDMA arrangement [3]. At the transmitter side, the binary data stream having a bit duration of T_b is serial-to-parallel converted to U parallel substreams. The new bit duration of each substream or the symbol duration is $T_s = UT_b$. After serial-to-parallel conversion, the uth substream modulates a subcarrier frequency f_u using binary phase shift keying (BPSK) for $u = 1, 2, \ldots, U$. Then, the U subcarrier-modulated substreams are added in order to form the complex modulated signal. Finally, spectral spreading is imposed on the complex signal by multiplying it with a spreading code. Therefore, the transmitted signal of user k can be expressed as

$$s_k(t) = \sum_{u=1}^{U} \sqrt{2P} b_{ku}(t) c_k(t) \cos(2\pi f_u t + \phi_{ku}) \qquad (3)$$

where P represents the transmitted power per subcarrier, while $\{b_{ku}(t)\}$, $c_k(t)$, $\{f_u\}$, and $\{\phi_{ku}\}$ represent the data stream, the DS spreading waveform, the subcarrier frequency set and the phase angles introduced in the carrier modulation process. The data stream's waveform $b_{ku}(t) = \sum_{i=-\infty}^{\infty} b_{ku} P_{T_s}(t - iT_s)$ consists of a sequence of mutually independent rectangular pulses of duration T_s and of amplitude $+1$ or -1 with equal probability. The spreading sequence $c_k(t) = \sum_{j=-\infty}^{\infty} c_{kj} P_{T_c}(t - jT_c)$ denotes the signature sequence waveform of the kth user, where c_{kj} assumes values of $+1$ or -1 with equal probability,

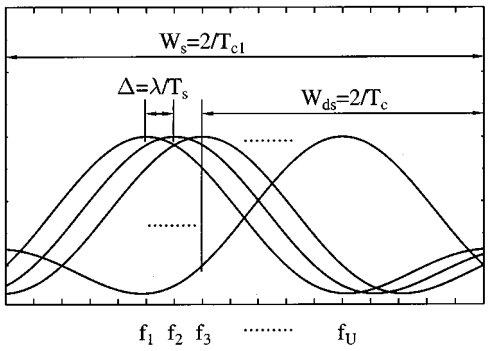

Fig. 2. Stylized spectrum of the overlapping MC DS-CDMA signals.

while $P_{T_c}(t)$ is the rectangular chip waveform, which is defined over the interval $[0, T_c)$.

The spectrum of the generalized MC DS-CDMA signal is shown in Fig. 2, where $W_s = 2/T_{c1}$ is the total bandwidth of the system, T_{c1} represents the chip-duration of a corresponding single-carrier DS-CDMA signal, while W_{ds} represents the "null-to-null" bandwidth of the subcarrier signals. The spacing between two adjacent subcarrier frequencies is assumed to be $\Delta = \lambda/T_s$, where again λ indicates the normalized spacing. Finally, the subcarrier frequencies in Fig. 2 are arranged according to

$$f_u = f_0 + \frac{\lambda(1-U+u)}{2T_s}, \qquad u = 0, 2, 4, \ldots, 2(U-1). \tag{4}$$

Let $N_e = T_s/T_c$ be the spreading gain of the subcarrier signals in the generalized MC DS-CDMA system and $N_1 = T_b/T_{c1}$ be the spreading gain of a corresponding single-carrier DS-CDMA system. Then, according to Fig. 2, the system's total transmission bandwidth, the subcarrier spacing Δ, and the DS spreading bandwidth of the subcarrier signal obey the relationship of $W_s = (U-1)\Delta + W_{ds}$, or

$$\frac{2}{T_{c1}} = (U-1)\frac{\lambda}{T_s} + \frac{2}{T_c}. \tag{5}$$

Multiplying both sides of the above equation by the symbol duration, T_s, and taking into account that $T_s = N_e T_c$ as well as that $T_s = UT_b = UN_1T_{c1}$, the processing gain, N_e, of the subcarrier signal can be expressed as

$$N_e = UN_1 - \frac{(U-1)\lambda}{2} \tag{6}$$

which implies that, for a given total system bandwidth of $W_s = 2/T_{c1}$ and for a given number of subcarriers U, N_e decreases as λ increases.

Fig. 3 shows the baseband equivalent power spectral density of the transmitted signal of (3) versus the normalized spacing λ, and the normalized frequency fT_{c1} for the parameters of $U = 8$, $N_1 = 64$. The power spectral density surface shows that, the transmitted signal's energy is concentrated near the center frequency, when the normalized spacing is low. By contrast, it spreads over the whole frequency band when the normalized spacing is high. Furthermore, it can be seen that there exist normalized spacing values, which spread the transmitted signal's energy uniformly over the valid frequency band. Since

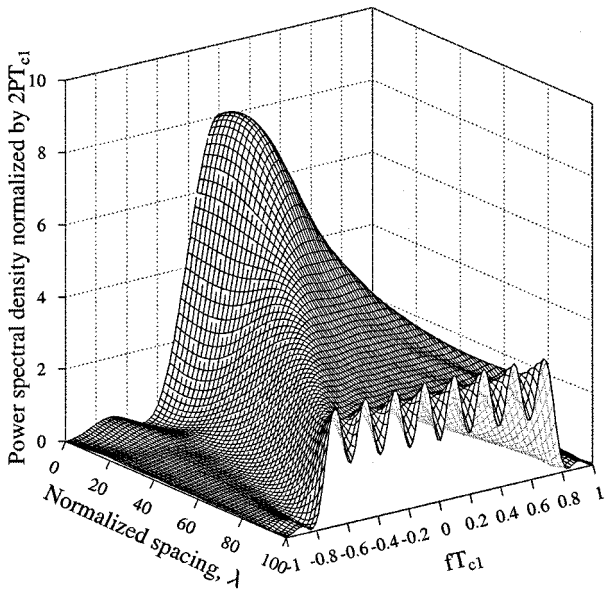

Fig. 3. Baseband equivalent power spectral density of the transmitted signal seen in (3) in the generalized MC DS-CDMA systems.

the power spectral density of the generalized MC DS-CDMA signals is a function of the spacing between the subcarriers, the power spectral density can be re-shaped during transmissions according to the prevalent system requirements, in order to maximize the achievable spectral efficiency by adjusting the spacing of the subcarriers.

B. Channel Model

We assume that the channel between the kth transmitter and the corresponding receiver is a multipath Nakagami-m fading channel [15]. The complex low-pass equivalent representation of the impulse response experienced by subcarrier u of user k is given by [28]

$$h_{ku}(t) = \sum_{l_p=0}^{L_p-1} \alpha_{ul_p}^{(k)} \delta(t - \tau_{kl_p}) \exp\left(-j\psi_{ul_p}^{(k)}\right) \tag{7}$$

where $\alpha_{ul_p}^{(k)}$, τ_{kl_p} and $\psi_{ul_p}^{(k)}$ represent the attenuation factor, delay and phase-shift for the l_pth multipath component of the channel, respectively, while L_p is the total number of diversity paths and $\delta(t)$ is the Kronecker-Delta function. Let T_m be the maximum delay spread of the communication channel. Then, the number of resolvable paths, L_p, associated with the generalized MC DS-CDMA signal is given by $L_p = \lfloor T_m/T_c \rfloor + 1$ [4], where $\lfloor x \rfloor$ represents the largest integer not exceeding x. The number of resolvable paths, L_1, in the context of the corresponding single-carrier DS-CDMA signal is given by $L_1 = \lfloor T_m/T_{c1} \rfloor + 1$. Multiplying both sides of (5) by T_m, we obtain that L_p and L_1 are related by

$$L_p \approx \left\lfloor \frac{2N_e(L_1-1)}{2N_e + (U-1)\lambda} \right\rfloor + 1. \tag{8}$$

We assume that the phases $\{\psi_{ul_p}^{(k)}\}$ in (7) are independent identically distributed (i.i.d.) random variables uniformly distributed in the interval $[0, 2\pi)$, while the L_p multipath attenuations

$\{\alpha_{ul_p}^{(k)}\}$ in (7) are independent Nakagami random variables with a probability density function (pdf) of [15], [19]–[23]

$$p\left(\alpha_{ul_p}^{(k)}\right) = M\left(\alpha_{ul_p}^{(k)}, m, \Omega_{ul_p}^{(k)}\right),$$
$$M(R, m, \Omega) = \frac{2m^m R^{2m-1}}{\Gamma(m)\Omega^m} e^{(-m/\Omega)R^2} \tag{9}$$

where $\Gamma(\cdot)$ is the gamma function [28], and m is the Nakagami-m fading parameter, which is equal to $m = E^2[(\alpha_{ul_p}^{(k)})^2]/\mathrm{Var}[(\alpha_{ul_p}^{(k)})^2]$. The parameter m of the amplitude distribution characterizes the severity of the fading over the l_pth resolvable path [22]. Specifically, $m = 1$ represents Rayleigh fading, $m \to \infty$ corresponds to the conventional Gaussian scenario, and $m = 1/2$ describes the so-called one-side Gaussian fading, i.e., the worst-case fading condition. The Rician and lognormal distributions can also be closely approximated by the Nakagami distribution in conjunction with $m > 1$ values. For more detailed information concerning the Nakagami distribution, readers are referred to the excellent overview by Simon and Alouini [20]–[22]. The parameter $\Omega_{ul_p}^{(k)}$ in (8) is the second moment of $\alpha_{ul_p}^{(k)}$, i.e., $\Omega_{ul_p}^{(k)} = E[(\alpha_{ul_p}^{(k)})^2]$. We assume a negative exponentially decaying multipath intensity profile (MIP) distribution given by $\Omega_{ul_p}^{(k)} = \Omega_{u0}^{(k)} \exp(-\eta l_p)$, $\eta \geq 0$, where $\Omega_{u0}^{(k)}$ is the average signal strength corresponding to the first resolvable path and η is the rate of average power decay.

Assuming K asynchronous CDMA users in the system, where all of them use the same U and N_e values, the average power received from each user at the base station is also assumed to be the same, implying perfect power control. Consequently, when K signals obeying the form of (3) are transmitted over the frequency-selective fading channels characterized by (7), the received signal at the base station can be expressed as

$$r(t) = \sum_{k=1}^{K}\sum_{u=1}^{U}\sum_{l_p=0}^{L_p-1} \sqrt{2P}\alpha_{ul_p}^{(k)} b_{ku}(t-\tau_{kl_p}) c_k(t-\tau_{kl_p}) \cdot \cos\left(2\pi f_u t + \varphi_{ul_p}^{(k)}\right) + n(t) \tag{10}$$

where $\varphi_{ul_p}^{(k)} = \phi_{ku} - \psi_{ul_p}^{(k)} - 2\pi f_u \tau_{kl_p}$, which is assumed to be an i.i.d. random variable having a uniform distribution in $[0, 2\pi)$, while $n(t)$ represents the additive white Gaussian noise (AWGN) with zero mean and double-sided power spectral density of $N_0/2$.

C. Receiver Model

Let the first user be the user-of-interest and consider the correlator-based RAKE receiver in conjunction with maximum ratio combining (MRC), as shown in Fig. 4, where the superscript and subscript of the reference user's signal has been omitted for notational convenience. In Fig. 4, L, $1 \leq L \leq L_p$, represents the number of diversity branches used by the receiver. We assume that the receiver is capable of acquiring perfect time-domain synchronization with each path of the reference signal. The multipath attenuations and phases are assumed to be perfect estimates of the channel parameters. Consequently, referring to Fig. 4, after MRC the decision variable Z_v of the zeroth data bit

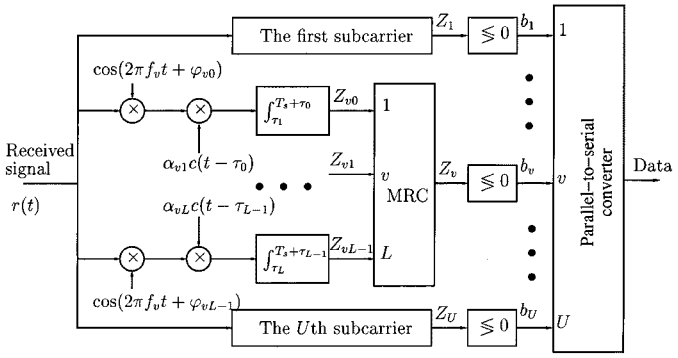

Fig. 4. Receiver block diagram of the generalized multicarrier DS-CDMA system.

corresponding to the vth substream of the reference user can be expressed as

$$Z_v = \sum_{l=0}^{L-1} Z_{vl}, \qquad v = 1, 2, \ldots, U \tag{11}$$

$$Z_{vl} = \int_{\tau_l}^{T_s+\tau_l} r(t) \cdot \alpha_{vl} c(t-\tau_l) \cos(2\pi f_v t + \varphi_{vl})\, dt. \tag{12}$$

Based on the decision variable Z_v, $v = 1, 2, \ldots, U$, the current data bit of the vth substream is decided to be 0 or 1, depending on whether Z_v is higher than zero. Finally, the U number of parallel data substreams are parallel-to-serial converted, in order to output the serial data bits. Let us now analyze the statistics of the decision variables.

III. Decision Variable Statistics

In this section, we analyze the statistics of the decision variable of Z_v. Without loss of generality, in the following analysis we let $\tau_l = 0$ in (12) for simplicity. Upon substituting (10) into (12), it can be shown that Z_{vl} can be written as

$$Z_{vl} = \sqrt{\frac{P}{2}} T_s \left\{ D_{vl} + N_{vl} + \sum_{\substack{l_p=0 \\ l_p \neq l}}^{L_p-1} I_1^{(s)} + \sum_{\substack{u=1 \\ u \neq v}}^{U}\sum_{l_p=0}^{L_p-1} I_2^{(s)} + \sum_{k=2}^{K}\sum_{l_p=0}^{L_p-1} I_1^{(k)} + \sum_{k=2}^{K}\sum_{\substack{u=1 \\ u \neq v}}^{U}\sum_{l_p=0}^{L_p-1} I_2^{(k)} \right\} \tag{13}$$

where N_{vl} is contributed by $n(t)$ of (10), which is a Gaussian random variable with zero mean and variance $\alpha_{vl}^2 N_0/2E_b$, where $E_b = PT_s$ represents the energy per bit. Furthermore, D_{vl} in (13) is the desired output derived by substituting (10) into (12) and setting $k = 1$, $l_p = l$ and $u = v$. Then D_{vl} can be written as $D_{vl} = b_v[0]\alpha_{vl}^2$. The output of the correlator matched to the vth subcarrier, lth path, and the reference user associated with $k = 1$ contains four types interference in (13). The interference term of $I_1^{(s)}$ is contributed by the path l_p, $l_p = 0, 1, \ldots, L_p - 1$ and $l_p \neq l$, associated with the same subcarrier v as the reference user, which can be expressed as

$$I_1^{(s)} = \frac{\alpha_{vl_p}\alpha_{vl}\cos\theta_{vl_p}}{T_s}\left[b_v[-1]R_1(\tau_{l_p}) + b_v[0]\hat{R}_1(\tau_{l_p})\right] \tag{14}$$

where $\theta_{vl_p} = \varphi_{vl_p} - \varphi_{vl}$, which is a random variable uniformly distributed in $[0, 2\pi)$, while $R_1(\tau_{l_p})$ and $\hat{R}_1(\tau_{l_p})$ are partial auto-correlation functions, which are defined as

$$R_1(\tau_{l_p}) = \int_0^{\tau_{l_p}} c(t-\tau_{l_p})c(t)\,dt \tag{15}$$

$$\hat{R}_1(\tau_{l_p}) = \int_{\tau_{l_p}}^{T_s} c(t-\tau_{l_p})c(t)\,dt. \tag{16}$$

The interference term of $I_2^{(s)}$ is contributed by the path l_p, $l_p = 0, \ldots, L_p - 1$, $l_p \neq l$, associated with the subcarriers u, $u = 1, 2, \ldots, U$, $u \neq m$ induced by the reference user,[1] which can be expressed as

$$I_2^{(s)} = \frac{\alpha_{ul_p}\alpha_{vl}}{T_s}\Big[b_u[-1]R_1(\tau_{l_p}, \theta_{ul_p}) + b_u[0]\hat{R}_1(\tau_{l_p}, \theta_{ul_p})\Big] \tag{17}$$

where $\theta_{ul_p} = \varphi_{ul_p} - \varphi_{vl}$. Due to the difference of the frequencies f_u and f_v associated with the subcarriers u and v, the corresponding partial autocorrelation functions are now defined as

$$R_1(\tau_{l_p}, \theta_{ul_p}) = \int_0^{\tau_{l_p}} c(t-\tau_{l_p})c(t)\cos(2\pi(f_u - f_v)t + \theta_{ul_p})\,dt \tag{18}$$

$$\hat{R}_1(\tau_{l_p}, \theta_{ul_p}) = \int_{\tau_{l_p}}^{T_s} c(t-\tau_{l_p})c(t)\cos(2\pi(f_u - f_v)t + \theta_{ul_p})\,dt. \tag{19}$$

With the aid of (4) we can rewrite (18) and (19) as

$$R_1(\tau_{l_p}, \theta_{ul_p}) = \int_0^{\tau_{l_p}} c(t-\tau_{l_p})c(t)\cos\left(\frac{2\pi\lambda(u-v)t}{T_s} + \theta_{ul_p}\right)dt \tag{20}$$

$$\hat{R}_1(\tau_{l_p}, \theta_{ul_p}) = \int_{\tau_{l_p}}^{T_s} c(t-\tau_{l_p})c(t)\cos\left(\frac{2\pi\lambda(u-v)t}{T_s} + \theta_{ul_p}\right)dt. \tag{21}$$

The multiuser interference (MUI) term $I_1^{(k)}$ in (13) is due to the path l_p, $l_p = 0, 1, \ldots, L_p - 1$ associated with the same subcarrier v engendered by the interfering users, $k = 2, \ldots, K$, which can be expressed as

$$I_1^{(k)} = \frac{\alpha_{vl_p}^{(k)}\alpha_{vl}\cos\theta_{vl_p}^{(k)}}{T_s}\Big[b_{kv}[-1]R_k(\tau_{kl_p}) + b_{kv}[0]\hat{R}_k(\tau_{kl_p})\Big] \tag{22}$$

where $\theta_{vl_p}^{(k)} = \varphi_{vl_p}^{(k)} - \varphi_{vl}$ is a random variable uniformly distributed in $[0, 2\pi)$, while $R_k(\tau_{kl_p})$ and $\hat{R}_k(\tau_{kl_p})$ are partial cross-correlation functions defined as

$$R_k(\tau_{kl_p}) = \int_0^{\tau_{kl_p}} c_k(t-\tau_{kl_p})c(t)\,dt \tag{23}$$

$$\hat{R}_k(\tau_{kl_p}) = \int_{\tau_{kl_p}}^{T_s} c_k(t-\tau_{kl_p})c(t)\,dt. \tag{24}$$

[1]Due to the orthogonality of the subcarrier signals received over the same path and from the same user, we have $\int_0^{T_s}\cos(2\pi f_i + \varphi_{il_p})\cos(2\pi f_j + \varphi_{jl_p})\,dt = 0$. Therefore, the interference term of $I_2^{(s)}$ due to the path l on the subcarrier u, $u = 1, 2, \ldots, U$, $u \neq v$ engendered by the reference user is zero. Hence, the associated terms are excluded by letting $l_p \neq l$ in (12).

Finally, the MUI term $I_2^{(k)}$ in (13) is due to the path l_p, $l_p = 0, \ldots, L_p - 1$ induced by the subcarrier u, $u = 1, \ldots, U$ and $u \neq v$ of the interfering user k, $k = 2, \ldots, K$, which can be expressed as

$$I_2^{(k)} = \frac{\alpha_{ul_p}^{(k)}\alpha_{vl}}{T_s}\Big[b_{ku}[-1]R_k\Big(\tau_{kl_p}, \theta_{ul_p}^{(k)}\Big) + b_{ku}[0]\hat{R}_k\Big(\tau_{kl_p}, \theta_{ul_p}^{(k)}\Big)\Big] \tag{25}$$

where $\theta_{ul_p}^{(k)} = \varphi_{ul_p}^{(k)} - \varphi_{vl}$ is a random variable uniformly distributed in $[0, 2\pi)$. The associated partial cross-correlation functions in (25) are defined as

$$R_k(\tau_{kl_p}, \theta_{ul_p}^{(k)}) = \int_0^{\tau_{kl_p}} c_k(t-\tau_{kl_p})c(t)\cos\left(\frac{2\pi\lambda(u-v)t}{T_s} + \theta_{ul_p}^{(k)}\right)dt \tag{26}$$

$$\hat{R}_k(\tau_{kl_p}, \theta_{ul_p}^{(k)}) = \int_{\tau_{kl_p}}^{T_s} c_k(t-\tau_{kl_p})c(t)\cos\left(\frac{2\pi\lambda(u-v)t}{T_s} + \theta_{ul_p}^{(k)}\right)dt. \tag{27}$$

Having analyzed the interference terms in (13), let us now consider the statistics of these interference contributions by assuming random spreading sequences and employing the standard Gaussian approximation [29]. According to (14), (17), (22), and (25), $I_1^{(s)}$, $I_2^{(s)}$, and $I_1^{(k)}$ constitute special cases of $I_2^{(k)}$. Specifically, if we set $u = v$ in (25), we obtain (22). If we let $k = 1$ in (25), then we get (17). Finally, if we let $k = 1$ and $u = v$, then we obtain (14). Hence, we can analyze the multipath interference engendered by the reference user as well as the MUI induced by the kth user by first analyzing the MUI of (25). Based on the standard Gaussian approximation [29], [30], the MUI term $I_2^{(k)}$ of (25) can be approximated as a Gaussian random variable with zero mean and variance given by

$$\mathrm{Var}\Big[I_2^{(k)}\Big] = \frac{\Omega_{ul_p}^{(k)}\alpha_{vl}^2}{T_s^2}\Big\{E_{\tau_{kl_p},\theta_{ul_p}^{(k)}}\Big[R_k^2\Big(\tau_{kl_p}, \theta_{ul_p}^{(k)}\Big)\Big] + E_{\tau_{kl_p},\theta_{ul_p}^{(k)}}\Big[\hat{R}_k^2\Big(\tau_{kl_p}, \theta_{ul_p}^{(k)}\Big)\Big]\Big\} \tag{28}$$

where $\Omega_{ul_p}^{(k)} = E[(\alpha_{ul_p}^{(k)})^2]$, while the second central moments of $R_k(\tau_{kl_p}, \theta_{ul_p}^{(k)})$ and $\hat{R}_k(\tau_{kl_p}, \theta_{ul_p}^{(k)})$—which were defined in (26) and (27)—with respect to τ_{kl_p} and $\theta_{ul_p}^{(k)}$ can be derived from [30, eqs. (35) and (36)][2] by setting $G = N_e$ and $x\Delta = \hat{x}\Delta = ((u-v)\lambda)/T_s$. It can be shown that

$$E_{\tau_{kl_p},\theta_{ul_p}^{(k)}}\Big[R_k^2\Big(\tau_{kl_p}, \theta_{ul_p}^{(k)}\Big)\Big] = E_{\tau_{kl_p},\theta_{ul_p}^{(k)}}\Big[\hat{R}_k^2\Big(\tau_{kl_p}, \theta_{ul_p}^{(k)}\Big)\Big] = \frac{N_e T_s^2}{4\pi^2(u-v)^2\lambda^2}\left[1 - \mathrm{sinc}\left(\frac{2\pi(u-v)\lambda}{N_e}\right)\right]. \tag{29}$$

[2]Typing errors: In [30, eqs. (35) and (36)], π should be replaced by π^2.

Upon substituting (29) into (28), it can be shown that the variance of $I_2^{(k)}$ can be expressed as

$$\mathrm{Var}\left[I_2^{(k)}\right] = \frac{\Omega_{ul_p}^{(k)}\alpha_{vl}^2 N_e}{2\pi^2(u-v)^2\lambda^2}\left[1-\mathrm{sinc}\left(\frac{2\pi(u-v)\lambda}{N_e}\right)\right]. \tag{30}$$

Let $u-v=x$ and compute the limit of $\lim_{x\to 0}\mathrm{Var}[I_2^{(k)}]$. We find that the variance of the interference term $I_2^{(k)}$ equals to $\Omega_{vl_p}^{(k)}\alpha_{vl}^2/3N_e$, which physically represents the interference power, when a subcarrier signal of the reference user is completely overlapping with the corresponding subcarrier signal of the kth interfering user, inflicting the interference variance of $I_1^{(k)}$ given by (22). Consequently, the MUI $I_1^{(k)}$ can be approximated as a Gaussian random variable with zero mean and variance given by

$$\mathrm{Var}\left[I_1^{(k)}\right] = \frac{\Omega_{vl_p}^{(k)}\alpha_{vl}^2}{3N_e}. \tag{31}$$

Upon using a similar approach to that invoked above for the computation of $I_2^{(k)}$, we can derive the variance of $I_2^{(s)}$ and the corresponding result is the same as that in (30) for $k=1$. This result is predictable, since random spreading sequences were assumed and each chip is assumed to be an i.i.d. random variable. Hence, the self-interference term of $I_2^{(s)}$ can be approximated as a Gaussian random variable with zero mean and variance given by

$$\mathrm{Var}\left[I_2^{(s)}\right] = \frac{\Omega_{ul_p}\alpha_{vl}^2 N_e}{2\pi^2(u-v)^2\lambda^2}\left[1-\mathrm{sinc}\left(\frac{2\pi(u-v)\lambda}{N_e}\right)\right]. \tag{32}$$

Finally, the self-interference term of $I_1^{(s)}$ can be approximated as a Gaussian random variable with zero mean. Its variance can be obtained from (32) by computing the limit of $\lim_{x=u-v\to 0}(\mathrm{Var}[I_2^{(s)}])$, which results in

$$\mathrm{Var}\left[I_1^{(s)}\right] = \frac{\Omega_{vl_p}\alpha_{vl}^2}{3N_e}. \tag{33}$$

Consequently, the correlator output Z_{vl} of (13) can be approximated as a Gaussian random variable with normalized mean given by $D_{vl} = b_v[0]\alpha_{vl}^2$ and normalized variance expressed as

$$\mathrm{Var}[Z_{vl}] = \left\{ \frac{\alpha_{vl}^2 N_0}{2E_b} + \sum_{\substack{l_p=0\\ l_p\neq l}}^{L_p-1}\mathrm{Var}\left[I_1^{(s)}\right] + \sum_{\substack{u=1\\ u\neq v}}^{U}\sum_{\substack{l_p=0\\ l_p\neq l}}^{L_p-1}\mathrm{Var}\left[I_2^{(s)}\right] + \sum_{k=2}^{K}\sum_{l_p=0}^{L_p-1}\mathrm{Var}\left[I_1^{(k)}\right] + \sum_{k=2}^{K}\sum_{\substack{u=1\\ u\neq v}}^{U}\sum_{l_p=0}^{L_p-1}\mathrm{Var}\left[I_2^{(k)}\right] \right\}. \tag{34}$$

Let $\overline{I}_s$ and $\overline{I}_M$ represent the average of $I_2^{(s)}$ and $I_2^{(k)}$ excluding the $\Omega_{ul_p}\alpha_{vl}^2$ multiplicative term in (32) and the $\Omega_{ul_p}^{(k)}\alpha_{vl}^2$ term in (30), respectively, with respect to v and u. Then it can be shown that

$$\begin{aligned}\overline{I}_s &= \overline{I}_M \\ &= \frac{1}{U(U-1)}\sum_{v=1}^{U}\sum_{\substack{u=1\\ u\neq v}}^{U}\frac{N_e}{2\pi^2(u-v)^2\lambda^2} \\ &\quad\cdot\left[1-\mathrm{sinc}\left(\frac{2\pi(u-v)\lambda}{N_e}\right)\right].\end{aligned} \tag{35}$$

We assume that the MIP is given by $\Omega_{ul_p}^{(k)} = \Omega_0\exp(-\eta l_p)$, the taps of which are independent variables for the subcarrier u and user k, i.e., we assume that all the subcarrier signals of the different users obey the same MIP distribution. Consequently, (34) can be expressed as

$$\begin{aligned}\mathrm{Var}[Z_{ml}] = \Bigg[&\left(\frac{2\Omega_0 E_b}{N_0}\right)^{-1} + \frac{(KL_p-1)q(L_p,\eta)}{L_p} \\ &\cdot\left(\frac{1}{3N_e}+(U-1)\overline{I}_M\right)\Bigg]\Omega_0\alpha_{vl}^2\end{aligned} \tag{36}$$

where $q(L_p,\eta) = (1-e^{-\eta L_p})/(1-e^{-\eta})$. Note that, in deriving (36), we also used $\Omega_{ul} = q(L_p,\eta)/L_p$, i.e., Ω_{ul} was replaced by its average value.

Since Z_v of (11) is the sum of L independent Gaussian random variables, Z_v is also a Gaussian random variable. The normalized mean of Z_v is given by

$$E[Z_v] = b_v[0]\sum_{l=0}^{L-1}\alpha_{vl}^2 \tag{37}$$

and the normalized variance of Z_v is given by

$$\begin{aligned}\mathrm{Var}[Z_v] = \Bigg[&\left(\frac{2\Omega_0 E_b}{N_0}\right)^{-1} + \frac{(KL_p-1)q(L_p,\eta)}{L_p} \\ &\cdot\left(\frac{1}{3N_e}+(U-1)\overline{I}_M\right)\Bigg]\cdot\Omega_0\sum_{l=0}^{L-1}\alpha_{vl}^2.\end{aligned} \tag{38}$$

Having obtained the statistics of the decision variables, in the following section we derive the average bit error rate (BER) for the generalized MC DS-CDMA system over multipath Nakagami-m fading channels.

IV. Performance Analysis

As we have argued in the above section, the decision variable, Z_v, $v=1, 2, \ldots, U$, can be approximated as a Gaussian random variable having a normalized mean given by (37) and a normalized variance given by (38). Therefore, the BER using BPSK modulation conditioned on a set of fading attenuations $\{\alpha_{vl}, l=0, 1, \ldots, L-1\}$ can be expressed as

$$P_b(\gamma) = Q\left(\sqrt{\frac{(E[Z_v])^2}{\mathrm{Var}[Z_v]}}\right) = Q\left(\sqrt{2\cdot\sum_{l=0}^{L-1}\gamma_l}\right) \tag{39}$$

where

$$\gamma_l = \gamma_c\cdot\frac{\alpha_{vl}^2}{\Omega_0} \tag{40}$$

$$\gamma_c = \left[\left(\frac{\Omega_0 E_b}{N_0} \right)^{-1} + \frac{2(KL_p - 1)q(L_p, \eta)}{L_p} \cdot \left(\frac{1}{3N_e} + (U-1)\bar{I}_M \right) \right]^{-1}. \quad (41)$$

Furthermore, in (39), $Q(x)$ represents the Gaussian Q-function, which is classically defined as [28]

$$Q(x) = \frac{1}{\sqrt{2\pi}} \int_x^\infty \exp\left(-\frac{t^2}{2}\right) dt.$$

Alternatively, the Gaussian Q-function can be represented as [20]–[22], [31]

$$Q(x) = \frac{1}{\pi} \int_0^{\pi/2} \exp\left(-\frac{x^2}{2\sin^2\theta}\right) d\theta, \qquad x \geq 0. \quad (42)$$

This representation has the advantage of having finite integration limits that are independent of the argument x and hence allows us to obtain a convenient analytical expression for the average BER of the multipath channel model, where the multipath channel outputs of $\{\gamma_l\}$ in (39) are not identically distributed [21], [22]. Classically, when using the conventional $Q(x)$ definition, the average BER is derived by first finding the pdf of $(2 \cdot \sum_{l=0}^{L-1} \gamma_l)$ in (39) and then averaging (39) over that pdf. However, it is difficult to find a simple expression for the pdf of $(2 \cdot \sum_{l=0}^{L-1} \gamma_l)$, when $\{\gamma_l\}_{l=0}^{L-1}$ obeys the same distribution but with different parameters, which is the case considered in this paper, since the average channel output SNR of $\bar{\gamma}_l = \gamma_c E[\alpha_{ml}^2]/\Omega_0 = \gamma_c \cdot e^{-\eta l}, l = 0, 1, \ldots, L-1$ depends on the multipath index of l. In [13], [19], and [32], the average BER of DS-CDMA systems has been analyzed over multipath Nakagami-m fading channels, using the conventional $Q(x)$ definition, where an approximated pdf of $(2 \cdot \sum_{l=0}^{L-1} \gamma_l)$ was considered. In the following analysis, we favor the alternative representation of (42) for the Gaussian Q-function without imposing any pdf approximation.

In order to obtain the average BER, P_b, we must average the conditional BER of (39) over the joint pdf of the instantaneous SNR sequence $\{\gamma_l\}_{l=0}^{L-1}$, namely, $p_{\gamma_0, \gamma_1, \ldots, \gamma_{L-1}}(\gamma_0, \gamma_1, \ldots, \gamma_{L-1})$. Since the random variables $\{\gamma_l\}_{l=0}^{L-1}$ are assumed to be statistically independent, we have $p_{\gamma_0, \gamma_1, \ldots, \gamma_{L-1}}(\gamma_0, \gamma_1, \ldots, \gamma_{L-1}) = \prod_{l=0}^{L-1} p_{\gamma_l}(\gamma_l)$, and the average BER can be expressed as

$$\begin{aligned} P_b &= \underbrace{\int_0^\infty \int_0^\infty \cdots \int_0^\infty}_{L\text{-fold}} Q\left(\sqrt{2 \cdot \sum_{l=0}^{L-1} \gamma_l}\right) \cdot \prod_{l=0}^{L-1} p_{\gamma_l}(\gamma_l) d\gamma_0 d\gamma_1 \cdots d\gamma_{L-1} \\ &= \underbrace{\int_0^\infty \int_0^\infty \cdots \int_0^\infty}_{L\text{-fold}} \frac{1}{\pi} \int_0^{\pi/2} \exp\left(-\frac{\sum_{l=0}^{L-1} \gamma_l}{\sin^2\theta}\right) d\theta \cdot \prod_{l=0}^{L-1} p_{\gamma_l}(\gamma_l) d\gamma_0 d\gamma_1 \cdots d\gamma_{L-1} \\ &= \frac{1}{\pi} \int_0^{\pi/2} \prod_{l=0}^{L-1} I_l(\bar{\gamma}_l, \theta)\, d\theta \end{aligned} \quad (43)$$

where

$$I_l(\bar{\gamma}_l, \theta) = \int_0^\infty \exp\left(-\frac{\gamma_l}{\sin^2\theta}\right) p_{\gamma_l}(\gamma_l)\, d\gamma_l. \quad (44)$$

Since $\gamma_l = \gamma_c \cdot (\alpha_{ml}^2/\Omega_0)$ and α_{ml} obeys the Nakagami-m distribution characterized by (9), it can be shown that the pdf of γ_l can be expressed as

$$p_{\gamma_l}(\gamma_l) = \left(\frac{m}{\bar{\gamma}_l}\right)^m \frac{\gamma^{m-1}}{\Gamma(m)} \exp\left(-\frac{m\gamma_l}{\bar{\gamma}_l}\right), \qquad \gamma_l \geq 0 \quad (45)$$

where $\bar{\gamma}_l = \gamma_c e^{-\eta l}$ for $l = 0, 1, \ldots, L-1$. Upon substituting (45) into (44), it can be shown that [22]

$$I_l(\bar{\gamma}_l, \theta) = \left(\frac{m\sin^2\theta}{\bar{\gamma}_l + m\sin^2\theta}\right)^m. \quad (46)$$

Finally, upon substituting (46) into (43), the average BER for the generalized MC DS-CDMA system considered can be expressed as

$$P_b = \frac{1}{\pi} \int_0^{\pi/2} \prod_{l=0}^{L-1} \left(\frac{m\sin^2\theta}{\bar{\gamma}_l + m\sin^2\theta}\right)^m d\theta. \quad (47)$$

In (47), since $(m\sin^2\theta/(\bar{\gamma}_l + m\sin^2\theta)) > 1$, it can be readily shown that the average BER decreases exponentially, when increasing the value of m, i.e., when the channel becomes better, while decreases approximately with the lth power of $m\sin^2\theta/(\bar{\gamma}_l + m\sin^2\theta)$, if $\bar{\gamma}_l$ is sufficiently similar for different MIP index values of l.

In addition to the analytical simplicity and accuracy, the power of using the alternative representation of the Gaussian Q-function in (42) and the convenience of the Nakagami-m distribution is also reflected by the general nature of the average BER expression of (47). Let us now consider some special cases.

A. Case 1: (Upper-Bound)

Since in (47)

$$\frac{m\sin^2\theta}{\bar{\gamma}_l + m\sin^2\theta} \leq \frac{m}{\bar{\gamma}_l + m}$$

it can be readily shown that

$$P_b \leq \frac{1}{2} \cdot \prod_{l=0}^{L-1} \left(\frac{m}{\bar{\gamma}_l + m}\right)^m. \quad (48)$$

B. Case 2: ($m \to \infty$)

The limit of (47) with respect to $m \to \infty$ can be written as

$$\begin{aligned} \lim_{m\to\infty} P_b &= \frac{1}{\pi} \int_0^{\pi/2} \prod_{l=0}^{L-1} \lim_{m\to\infty} \left(\frac{m\sin^2\theta}{\bar{\gamma}_l + m\sin^2\theta}\right)^m d\theta \\ &= \frac{1}{\pi} \int_0^{\pi/2} \prod_{l=0}^{L-1} \frac{d\theta}{\left[\lim_{m\to\infty} \left(1 + \frac{\bar{\gamma}_l}{m\sin^2\theta}\right)^{m\sin^2\theta/\bar{\gamma}_l}\right]^{\bar{\gamma}_l/\sin^2\theta}} \\ &= \frac{1}{\pi} \int_0^{\pi/2} \exp\left(-\frac{2 \cdot \sum_{l=0}^{L-1} \bar{\gamma}_l}{2\sin^2\theta}\right) d\theta \\ &= Q\left(\sqrt{2 \cdot \sum_{l=0}^{L-1} \bar{\gamma}_l}\right) \end{aligned} \quad (49)$$

where we used

$$\lim_{m\to\infty}\left(1+\frac{\overline{\gamma}_l}{m\sin^2\theta}\right)^{m\sin^2\theta/\overline{\gamma}_l}=e$$

in arriving from the second step to the third step. Since the channel attenuation factor α_{ml} in (40) is a constant, when $m\to\infty$, we have $\overline{\gamma}_l=\gamma_l$, which is also a constant. Therefore, as expected, (49) represents the system's BER over AWGN channels.

C. Case 3: ($\eta=0$)

When $\eta=0$, then each path has the same MIP distribution, which in turn means that $\{\gamma_l\}_{l=0}^{L-1}$ in (40) are i.i.d. random variables and $\overline{\gamma}_0=\overline{\gamma}_1=\cdots=\overline{\gamma}_{L-1}=\gamma_c$. Therefore, (47) can be expressed as

$$P_b=\frac{1}{\pi}\int_0^{\pi/2}\left(\frac{m\sin^2\theta}{\gamma_c+m\sin^2\theta}\right)^{mL}d\theta. \tag{50}$$

According to the analysis of Alouini and Goldsmith in [22, Appendix 2], (50) can be expressed in a closed form as

$$P_b=\sqrt{\frac{\gamma_c}{\gamma_c+m}}\,\frac{(1+\gamma_c/m)^{-mL}\Gamma(mL+1/2)}{2\sqrt{\pi}\Gamma(mL+1)}\times{}_2F_1\left(1,\,mL+\frac{1}{2};\,mL+1;\,\frac{m}{m+\gamma_c}\right) \tag{51}$$

where ${}_2F_1(a,\,b;\,c;\,z)$ is the hypergeometric function defined as [19]

$${}_2F_1(a,\,b;\,c;\,z)=\sum_{k=0}^{\infty}\frac{(a)_k(b)_kz^k}{(c)_kk!}$$

and $(a)_k=a(a+1)\cdots(a+k-1)$, $(a)_0=1$. Equation (51) is the BER expression derived in [19] by Eng and Milstein using the classical representation of the Gaussian Q-function. Moreover, if mL is a positive integer, then (51) can be reduced following Alouini and Goldsmith [22] to

$$P_b=\left[\frac{1-\mu}{2}\right]^{mL}\sum_{k=0}^{mL-1}\binom{mL-1+k}{k}\left[\frac{1+\mu}{2}\right]^k \tag{52}$$

where $\mu=\sqrt{\gamma_c/(\gamma_c+m)}$.

D. Case 4: ($\eta=0$, $m=1$)

When $\eta=0$, $m=1$, then the channel model represents the multipath Rayleigh fading channel and the multipath fading channel outputs are i.i.d. random variables. In this case, the average BER can be derived from (52) by setting $m=1$, yielding

$$P_b=\left[\frac{1-\mu}{2}\right]^{L}\sum_{k=0}^{L-1}\binom{L-1+k}{k}\left[\frac{1+\mu}{2}\right]^k \tag{53}$$

with $\mu=\sqrt{\gamma_c/(\gamma_c+1)}$. Then (53) represents the average BER of BPSK modulation given in [28, Eq. (14-4-15)] over the multipath Rayleigh fading channel. In summary, above we have analyzed the performance of the generalized multicarrier DS-CDMA system using BPSK modulation over generalized multipath Nakagami-m fading channels. Let us now evaluate the system's performance numerically.

V. Numerical Results

In this section we evaluate the performance of generalized multicarrier DS-CDMA, investigate the effect of the normalized subcarrier spacing, λ, on the system's performance, and compare the performance of MC DS-CDMA having the optimum spacing with that of multitone DS-CDMA [3] and orthogonal multicarrier DS-CDMA [5]. Note that all the BER results in this section were computed from (47). For convenience, the parameters common in all figures are summarized as follows. The spreading gain and the number of resolvable paths of the corresponding single-carrier DS-CDMA system are $N_1=128$ and $L_1=32$, respectively. The MIP decay-factor is $\eta=0.2$. Throughout this section, the number of subcarriers used is $U=2$, 4, 8, 16, and 32. The normalized subcarrier spacing for the multitone DS-CDMA system is $\lambda=1$. According to (6), the normalized subcarrier spacing for the orthogonal MC DS-CDMA system using the above number of subcarriers becomes $\lambda=N_e\approx 170$, 204, 227, 240, and 248, respectively.

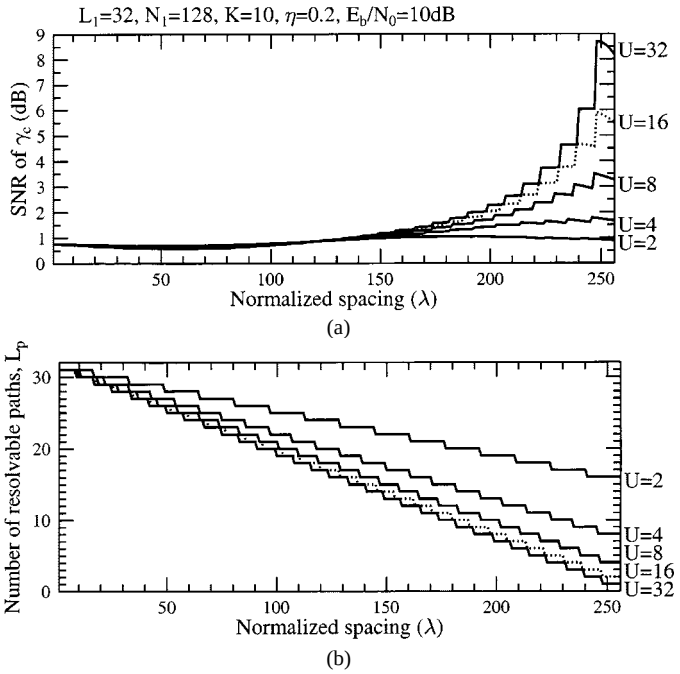

Fig. 5. The effect of the normalized subcarrier spacing λ (a) on the SNR γ_c, which is computed from (41) and (b) on the number of resolvable paths L_p, which is computed from (8), when the number of resolvable paths and the spreading gain of the corresponding single-carrier DS-CDMA system are $L_1=32$, $N_1=128$, respectively, the number of simultaneous users is $K=10$, the SNR per bit is $E_b/N_0=10$ dB, and the MIP decay-factor is $\eta=0.2$.

In Fig. 5, we demonstrate the mutual influence of the normalized subcarrier spacing, λ, on both the SNR γ_c of (41) [Fig. 5(a)] and on the number of resolvable paths, L_p of (8) [Fig. 5(b)]. Note that, since the number of resolvable paths according to (8) and the spreading gain according to (6) assume integer values, the curves are hence step-wise linear appear in the form of steps. From the results of Fig. 5(a), we observe that the SNR γ_c remains approximately constant over the range of $\lambda\in[1,\,150]$. However, for $\lambda>150$, the SNR of γ_c increases, when increasing the spacing, λ, if the number of subcarriers is higher than four. The number of resolvable paths in Fig. 5(b) decreases linearly upon increasing the spacing, λ.

Since the average BER will decrease, when the SNR γ_c is increased, and vice versa, the BER increases, when the number of resolvable paths is decreased. Therefore, according to Fig. 5, we can conclude that there exists an optimum value of λ, which will result in the minimum average BER. The influence of the

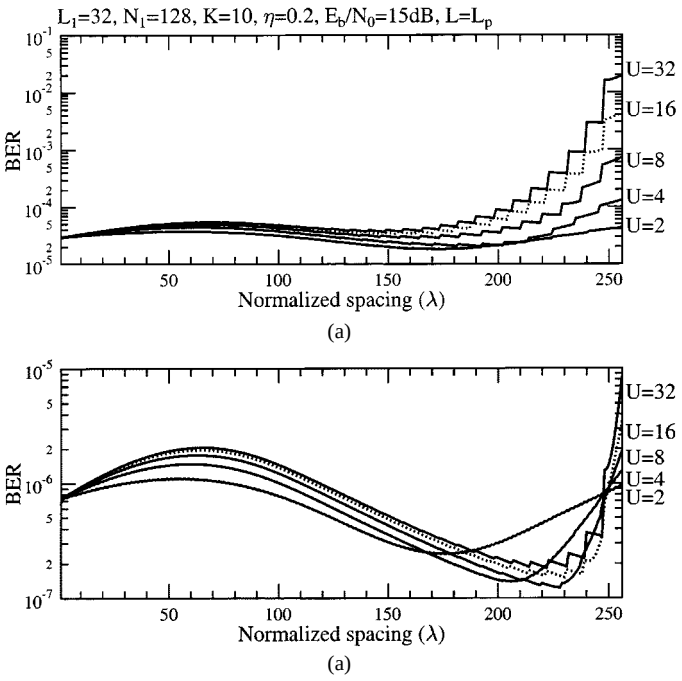

Fig. 6. BER versus the normalized subcarrier spacing, λ for the generalized MC DS-CDMA system over the multipath Nakagami-m fading channel, where (a) $m = 1$ represents the Rayleigh fading and (b) $m = 20$ models the Rician fading channel. The other parameters used in both figures are $L_1 = 32$, $N_1 = 128$, $K = 10$, $\eta = 0.2$, $E_b/N_0 = 15$ dB. The results were computed from (47) by assuming that $L = L_p$, i.e., the receiver was capable of combining all the resolvable paths.

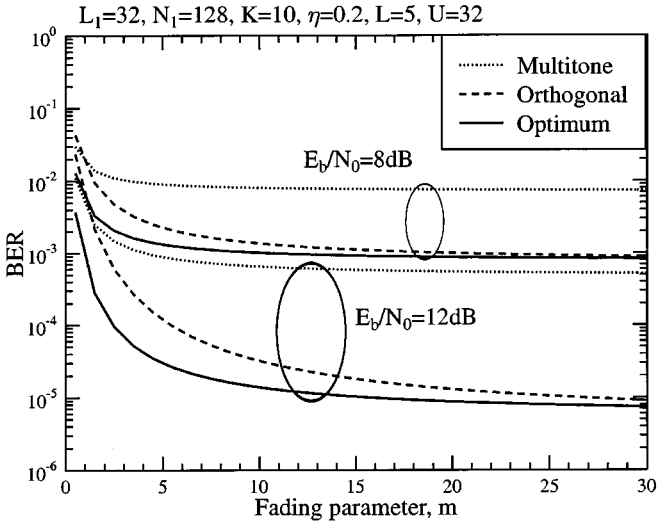

Fig. 7. BER versus the fading parameter, m, for the MC DS-CDMA having the optimum normalized subcarrier spacing, for the multitone DS-CDMA and the orthogonal MC DS-CDMA systems over multipath Nakagami-m fading channels using the parameters of $L_1 = 32$, $N_1 = 128$, $K = 10$, $\eta = 0.2$, $E_b/N_0 = 8$ dB and 15 dB. The results were computed from (47) by assuming that we had $L = 5$, i.e., that the receiver was capable of combining at most five resolvable paths.

normalized subcarrier spacing, λ, on the average BER of the generalized MC DS-CDMA system is shown explicitly in Fig. 6, where both the multipath Rayleigh fading channel associated with $m = 1$ [Fig. 6(a)] and the multipath Rician fading channel of $m = 20$ [Fig. 6(b)] were considered. From the results of Fig. 6(a), we infer that the BER of the multicarrier system using a given number of subcarriers changes slowly, when $\lambda < 200$, and there is no pronounced optimum spacing. In contrast to Fig. 6(a), in Fig. 6(b) the BER changes more explicitly, when changing the spacing λ. By carefully observing the curves in Fig. 6(b), we find that the optimum spacing for a given value of U was around $\lambda = N_e$, where the orthogonal MC DS-CDMA scheme achieves the best BER performance. In Fig. 6(a) and (b), we assumed that all the resolvable paths were combined in the receiver irrespective of the complexity. Hence, the complexity of the RAKE receiver decreases, when increasing the spacing λ, since the number of resolvable paths, L_p, decreases for all values of U, when increasing the spacing λ, as shown in Fig. 5(b). Therefore, from this point of view, the multitone DS-CDMA scheme associated with $\lambda = 1$ does not constitute a good design tradeoff, when compared to the orthogonal MC DS-CDMA scheme having a spacing of $\lambda \gg 1$, since it results in a higher receiver complexity without any commensurate BER benefits. This is true even over the Rayleigh fading scenario of Fig. 6(a), where the BER deficiency of the $\lambda = 1$ scenario is less obvious.

In Fig. 6, we assumed that the receiver was capable of combining all the resolvable paths. However, due to the maximum complexity constraint of the receiver, typically it can only combine a fraction of the resolvable paths. Hence, in the following figures we assumed that the receiver was capable of combining at most five resolvable paths, namely the first five resolvable paths having the highest average power, if we had $L_p > 5$, while it combined all the resolvable paths, if we had $L_p \leq 5$. This assumption tacitly implies that the RAKE receivers of the different MC DS-CDMA systems considered had the same complexity. From Fig. 7–10, the BER performance of multitone DS-CDMA, orthogonal multicarrier DS-CDMA, and MC DS-CDMA having optimum spacing—associated with the system that achieved the minimum BER—was characterized and compared.

In Fig. 7, the BER versus the fading parameter, m, was evaluated for the above-mentioned three types of multicarrier DS-CDMA schemes at $E_b/N_0 = 8$ dB and 12 dB. The channel models considered encompassed the range from the worst-case one-sided Gaussian fading channel associated with $m = 1/2$ to the high-quality, asymptotically AWGN channel of $m = 30$. From the results of Fig. 7, we observe that the multitone DS-CDMA scheme marginally outperforms the orthogonal MC DS-CDMA scheme, when the channel fading is extremely severe, such as in the case of $m = 1/2$, and $m = 1$. However, if the channel quality is sufficiently high ($m > 1$), the multitone DS-CDMA scheme is outperformed by the orthogonal MC DS-CDMA scheme. Furthermore, it can be observed that for the cases considered neither the multitone DS-CDMA nor the orthogonal MC DS-CDMA are optimum schemes. More explicitly, from the results we infer that for any given value of m there exists an optimum spacing of $1 < \lambda < N_e$, which results in a minimum-BER MC DS-CDMA scheme that outperforms both the multitone DS-CDMA and the orthogonal MC DS-CDMA systems. However, the BER of orthogonal MC DS-CDMA converges to that of the optimum multicarrier DS-CDMA scheme in Fig. 7, when the channel quality characterized by the fading parameter m improves. This observation implies that the orthogonal multicarrier DS-CDMA arrangement represents the asymptotically optimum scheme, when m is sufficiently high.

In Figs. 8 and 9, the BER versus E_b/N_0 performance was evaluated in the context of the multitone, the orthogonal multicarrier and the "spacing-optimized" MC DS-CDMA

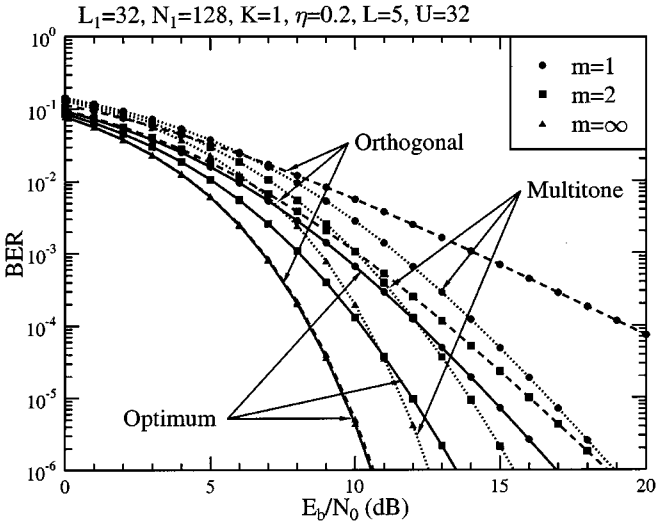

Fig. 8. BER versus the SNR per bit, E_b/N_0, performance for the MC DS-CDMA system having the optimum normalized subcarrier spacing, for the multitone DS-CDMA and for the orthogonal MC DS-CDMA systems over the multipath Nakagami-m fading channel using parameters of $L_1 = 32$, $N_1 = 128$, $K = 1$, $\eta = 0.2$, $m = 1, 2$ and ∞. The results were computed from (47) by assuming that we had $L = 5$, i.e., the receiver was only capable of combining at most five resolvable paths.

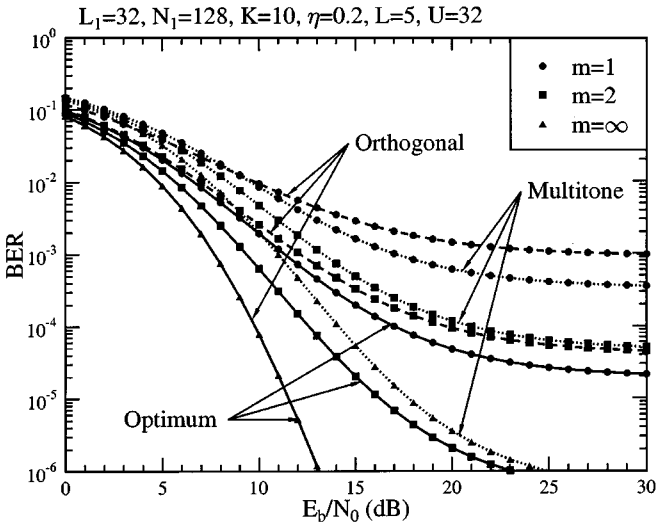

Fig. 9. BER versus the SNR per bit, E_b/N_0, performance for the MC DS-CDMA system having the optimum normalized subcarrier spacing, for the multitone DS-CDMA and for the orthogonal MC DS-CDMA systems over the multipath Nakagami-m fading channel using parameters of $L_1 = 32$, $N_1 = 128$, $K = 10$, $\eta = 0.2$, $m = 1, 2$ and ∞. The results were computed from (47) by assuming that we had $L = 5$, i.e., the receiver was only capable of combining at most five resolvable paths.

schemes for $m = 1$, 2 and ∞. The parameters employed in the context of both figures were the same, except that in Fig. 8 the number of users was one, which characterizes the performance of a system using ideal multiuser detection, while in Fig. 9, the number of users was 10. The other parameters were shown at the top of the figures. From these results, we find that when $m = 1$ and $E_b/N_0 > 6$ dB for $K = 1$, while $E_b/N_0 > 8$ dB for $K = 10$, and when $m = 2$ and $E_b/N_0 > 10.5$ dB, the multitone DS-CDMA scheme outperforms the orthogonal MC DS-CDMA arrangement, but for any other scenarios orthogonal MC DS-CDMA marginally outperforms multitone DS-CDMA. However, both the multitone and the orthogonal

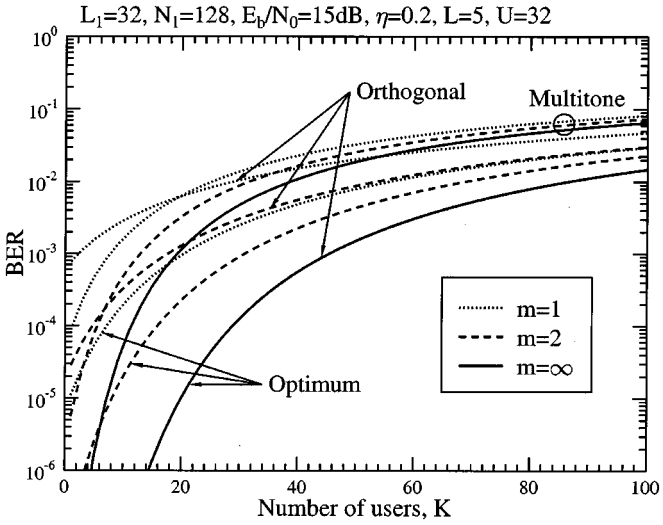

Fig. 10. BER versus the number of users, K, for the MC DS-CDMA having the optimum normalized subcarrier spacing, for the multitone DS-CDMA and for the orthogonal MC DS-CDMA systems over the multipath Nakagami-m fading channel using parameters of $L_1 = 32$, $N_1 = 128$, $E_b/N_0 = 15$ dB, $\eta = 0.2$, $m = 1, 2$ and ∞. The results were computed from (47) by assuming that we had $L = 5$, i.e., the receiver was only capable of combining at most five resolvable paths.

multicarrier DS-CDMA schemes are outperformed by the "spacing-optimized" MC DS-CDMA scheme, when $m = 1$ and 2. For the AWGN channel of $m \to \infty$ both the orthogonal and the "spacing-optimized" MC DS-CDMA schemes achieve the very close BER performance at any SNR per bit value.

Finally, in Fig. 10, we evaluated the BER versus the number of active users, K, in the context of the multitone, orthogonal and "spacing-optimized" MC DS-CDMA schemes in terms of $m = 1$, 2 and ∞. According to the results we observe that when $m = 1$, 2 and $K < 20$, 6, respectively, then multitone DS-CDMA outperforms orthogonal MC DS-CDMA, but for any other cases, orthogonal MC DS-CDMA outperforms multitone DS-CDMA. However, both the multitone and the orthogonal MC DS-CDMA schemes are outperformed by the "spacing-optimized" MC DS-CDMA scheme, when $m = 1$ and 2. For the AWGN channel of $m \to \infty$ both the orthogonal multicarrier and the "spacing-optimized" MC DS-CDMA schemes achieve the same BER performance for any number of active users.

VI. Conclusion

In summary, in this contribution the performance of the generalized MC DS-CDMA system has been investigated. We have presented a unified analytical framework for determining the exact average BER of generalized MC DS-CDMA over the generalized multipath Nakagami-m fading channel. We have investigated the effect of the subcarrier spacing λ on the performance of the generalized MC DS-CDMA system. The BER performance of the "spacing-optimized" MC DS-CDMA scheme, the multitone DS-CDMA scheme as well as that of the orthogonal MC DS-CDMA scheme has been evaluated and compared. From the results, we inferred the following conclusions.

In the generalized MC DS-CDMA scheme, for a given system bandwidth and a given channel environment, there exists an optimum subcarrier spacing, which results in a minimum BER MC DS-CDMA system. In general, neither multitone

DS-CDMA nor orthogonal MC DS-CDMA can match the performance of the "spacing-optimized" MC DS-CDMA scheme. However, if the channel quality is sufficiently high, the orthogonal MC DS-CDMA scheme can asymptotically achieve the optimum BER performance. When AWGN channels are considered, the orthogonal MC DS-CDMA scheme represents the "spacing-optimized" MC DS-CDMA scheme.

ACKNOWLEDGMENT

The authors would like to acknowledge the contributions of their colleagues.

REFERENCES

[1] R. Prasad and S. Hara, "Overview of multicarrier CDMA," *IEEE Commun. Mag.*, pp. 126–133, Dec. 1997.

[2] V. M. Dasilva and E. S. Sousa, "Multicarrier orthogonal CDMA signals for quasisynchronous communication systems," *IEEE J. Select. Areas Commun.*, vol. 12, pp. 842–852, June 1994.

[3] L. Vandendorpe, "Multitone spread spectrum multiple access communications system in a multipath Rician fading channel," *IEEE Trans. Veh. Technol.*, vol. 44, pp. 327–337, 1995.

[4] S. Kondo and L. B. Milstein, "Performance of multicarrier DS CDMA systems," *IEEE Trans. Commun.*, vol. 44, pp. 238–246, Feb. 1996.

[5] E. A. Sourour and M. Nakagawa, "Performance of orthogonal multicarrier CDMA in a multipath fading channel," *IEEE Trans. Commun.*, vol. 44, pp. 356–367, Mar. 1996.

[6] X. Gui and T. S. Ng, "Performance of asynchronous orthogonal multicarrier CDMA system in frequency selective fading channel," *IEEE Trans. Commun.*, vol. 47, pp. 1084–1091, July 1999.

[7] S. Hara and R. Prasad, "Design and performance of multicarrier CDMA system in frequency-selective Rayleigh fading channels," *IEEE Trans. Veh. Technol.*, vol. 48, pp. 1584–1595, Sept. 1999.

[8] Y. H. Kim, I. Song, I. Seokho, and S. R. Park, "A multicarrier CDMA system with adaptive subchannel allocation for forward links," *IEEE Trans. Veh. Technol.*, vol. 48, pp. 1428–1436, Sept. 1999.

[9] B. J. Rainbolt and S. L. Miller, "Multicarrier CDMA for cellular overlay systems," *IEEE J. Select. Areas Commun.*, vol. 17, pp. 1807–1814, Oct. 1999.

[10] D. N. Rowitch and L. B. Milstein, "Convolutionally coded multicarrier DS-CDMA systems in a multipath fading channel—Part I: Performance analysis," *IEEE Trans. Commun.*, vol. 47, pp. 1570–1582, Oct. 1999.

[11] ——, "Convolutionally coded multicarrier DS-CDMA systems in a multipath fading channel—Part II: Narrow-band interference suppression," *IEEE Trans. Commun.*, vol. 47, pp. 1729–1736, Nov. 1999.

[12] L.-L. Yang and L. Hanzo, "Slow frequency-hopping multicarrier DS-CDMA," in *Int. Symp. on Wireless Personal Multimedia Communications (WPMC'99)*, Amsterdam, The Netherlands, Sept. 21–23, 1999, pp. 224–229.

[13] ——, "Blind joint soft-detection assisted slow frequency-hopping multicarrier DS-CDMA," *IEEE Trans. Commun.*, vol. 48, pp. 1520–1529, Sept. 2000.

[14] ——, "Slow frequency-hopping multicarrier DS-CDMA for transmission over Nakagami multipath fading channels," *IEEE J. Select. Areas Commun.*, vol. 19, pp. 1211–1221, July 2001.

[15] N. Nakagami, "The m-distribution, a general formula for intensity distribution of rapid fading," in *Statistical Methods in Radio Wave Propagation*, W. G. Hoffman, Ed. Oxford, U.K.: Pergamon, 1960.

[16] H. Xiang, "Binary code-division multiple-access systems operating in multipath fading, noise channels," *IEEE Trans. Commun.*, vol. COM-33, pp. 775–784, Aug. 1985.

[17] M. K. Simon and M.-S. Alouini, "A unified performance analysis of digital communication with dual selective combining diversity over correlated Rayleigh and Nakagami-m fading channels," *IEEE Trans. Commun.*, vol. 47, pp. 33–43, Jan. 1999.

[18] M.-S. Alouini and M. K. Simon, "Application of the Dirichlet transformation to the performance evaluation of generalized selection combining over Nakagami-m fading channels," *J. Commun. Networks*, vol. 47, pp. 5–13, Mar. 1999.

[19] T. Eng and L. B. Milstein, "Coherent DS-CDMA performance in Nakagami multipath fading," *IEEE Trans. Commun.*, vol. 43, pp. 1134–1143, Feb./Mar./Apr. 1995.

[20] M. K. Simon and M.-S. Alouini, "A unified approach to the probability of error for noncoherent and differentially coherent modulation over generalized fading channels," *IEEE Trans. Commun.*, vol. 46, pp. 1625–1638, Dec. 1998.

[21] ——, "A unified approach to the performance analysis of digital communication over generalized fading channels," *Proc. IEEE*, vol. 86, pp. 1860–1877, Sept. 1998.

[22] M.-S. Alouini and A. J. Goldsmith, "A unified approach for calculating error rates of linearly modulated signals over generalized fading channels," *IEEE Trans. Commun.*, vol. 47, pp. 1324–1334, Sept. 1999.

[23] V. Aalo, O. Ugweje, and R. Sudhakar, "Performance analysis of a DS/CDMA system with noncoherent M-ary orthogonal modulation in Nakagami fading," *IEEE Trans. Veh. Technol.*, vol. 47, pp. 20–29, Feb. 1998.

[24] Q. T. Zhang, "Exact analysis of postdetection combining for DPSK and NKSF systems over arbitrarily correlated Nakagami channels," *IEEE Trans. Commun.*, vol. 46, pp. 1459–1467, Nov. 1998.

[25] M. S. Alouini and M. K. Simon, "Performance of coherent receivers with hybrid SC/MRC over Nakagami-m fading channels," *IEEE Trans. Veh. Technol.*, vol. 48, pp. 1155–1164, July 1999.

[26] A. Annamalai, "Microdiversity reception of spread-spectrum signals on Nakagami fading channels," *IEEE Trans. Commun.*, vol. 47, pp. 1747–1756, Nov. 1999.

[27] S. W. Kim and Y. H. Lee, "Combined rate and power adaption in DS/CDMA communications over Nakagami fading channels," *IEEE Trans. Commun.*, vol. 48, pp. 162–168, Jan. 2000.

[28] J. G. Proakis, *Digital Communications*, 3rd ed. New York: McGraw-Hill, 1995.

[29] M. B. Pursley, "Performance evaluation for phase-coded spread-spectrum multiple-access communication—Part I: System analysis," *IEEE Trans. Commun.*, vol. COM-25, pp. 795–799, Aug. 1977.

[30] L.-L. Yang and L. Hanzo, "Overlapping M-ary frequency shift keying spread-spectrum multiple-access systems using random signature sequences," *IEEE Trans. Veh. Technol.*, vol. 48, pp. 1984–1995, Nov. 1999.

[31] M. K. Simon and D. Divsalar, "Some new twists to problems involving the Gaussian probability integral," *IEEE Trans. Commun.*, vol. 46, pp. 200–210, Feb. 1998.

[32] G. P. Efthymoglou, V. A. Aalo, and H. Helmken, "Performance analysis of coherent DS-CDMA system in a Nakagami fading channel with arbitrary parameters," *IEEE Trans. Veh. Tech.*, vol. 46, pp. 289–296, May 1997.

Lie-Liang Yang (M'98) received the B.Eng. degree in communication engineering from Shanghai TieDao University, Shanghai, China, in 1988 and the M.S. and Ph.D. degrees in communications and electronics from Northern Jiaotong University, Beijing, China, in 1991 and 1997, respectively.

From 1991 to 1993, he was a Lecturer in the Department of Electrical Engineering, East-China Jiaotong University, China. From 1993 to 1997 he was with the Modern Communications Research Institute, Northern Jiaotong University, China. From June 1997 to December 1997, he was a Visiting Scientist of the Institute of Radio Engineering and Electronics, Academy of Sciences of the Czech Republic. Since December 1997, he has been with the Communication Group, Department of Electronics and Computer Science, University of Southampton, U.K., and has been involved in researching various error-correction coding, modulation, and detection techniques, as well as wide-band, broad-band and ultrawide-band CDMA systems for the advanced wireless mobile communication systems. He has published over 60 papers in journals and conference proceedings.

Dr. Yang was awarded the Royal Society Sino-British Fellowship in 1997.

Lajos Hanzo (M'91–SM'92) graduated in electronics in 1976 and received the Ph.D. degree in 1983.

During his 25-year career in telecommunications, he has held various research and academic posts in Hungary, Germany, and the U.K. Since 1986, he has been with the Department of Electronics and Computer Science, University of Southampton, Southampton, U.K., and has been a consultant to Multiple Access Communications Ltd., U.K. Currently he holds the Chair of Telecommunications at the University of Southampton. He co-authored eight books on mobile radio communications, published more than 400 research papers, organized and chaired conference sessions, presented overview lectures, and was awarded a number of distinctions. His current research interests are in the field of wireless multimedia communications. His work is sponsored both by industry, the Engineering and Physical Sciences Research Council (EPSRC) U.K., the European IST Programme, and the Mobile Virtual Centre of Excellence (VCE), U.K.